Algorithmic Primitives for Quantum-Assisted Quantum Control

Guru-Vamsi Policharla[1] and Sai Vinjanampathy[1,2,*]
[1]Department of Physics, Indian Institute of Technology-Bombay, Powai, Mumbai 400076, India
[2]Centre for Quantum Technologies, National University of Singapore, 3 Science Drive 2, Singapore 117543, Singapore

(Received 7 December 2020; revised 10 August 2021; accepted 22 October 2021; published 23 November 2021)

We present two primitive algorithms to evaluate overlaps and transition matrix time series, which are then used to construct several quantum-assisted quantum control algorithms. Unlike previous approaches, our method bypasses tomographically complete measurements and instead relies solely on single qubit measurements. We analyze circuit complexity of composed algorithms and sources of noise arising from Trotterization and measurement errors.

DOI: 10.1103/PhysRevLett.127.220504

Introduction.—Quantum control is central to the design of quantum technologies [1]. The control problem usually involves optimizing a cost function that incorporates conditions such as distance to a target state, bandwidth, and fluence restrictions. The problem is then solved by employing gradient search methods [2–7], nongradient search methods [7–15], or hybrid algorithms [16,17]. Such solutions typically involve several iterative updates to the controls before convergence to a local optima. Since these methods simulate quantum evolution on a classical computer repeatedly, often the time complexity for many-body quantum control protocols is dominated by the corresponding complexity of simulating the evolution.

Several techniques to partially overcome the computational intractability have been developed. For instance, mean-field and cumulant expansion theories [18,19] have been used in the place of the full evolution. However, the approximations are either limited or uncontrolled. Another recent approach [20] has been to use matrix product state approaches embedded inside control algorithms. Though this simulates a larger set of quantum states on a classical computer, such techniques cannot efficiently simulate generic quantum evolution.

Given the advances in noisy intermediate-scale quantum (NISQ) computing [21,22] platforms, a potential solution is to simulate quantum evolution on NISQ devices [23] and extract control pulses via measurements. This problem has been considered before, though the solutions have been limited. For instance, the hybrid GRAPE algorithm was proposed [24,25] and implemented [26] for optimal control. The states are evolved on a quantum simulator and the cost function and its gradients are estimated by projecting the final density matrix into specific quantum states. This technique is limited by the fact that the number of projectors needed to span an arbitrary density matrix basis is exponential in the number of qubits. To mitigate this, previous authors typically restricted the target states to sparse matrices in the measurement basis, which in turn restricts the possible control solutions one can obtain.

In this Letter, we propose the first control solution for state optimization that is applicable to dense target states by adapting existing techniques from quantum computation and expanding them to compose two *algorithmic primitives*. They can be implemented on a universal quantum computer, provided the many-body target states are available as an off-line resource. This demand for an off-line resource is justified since our method is akin to compilation of quantum circuits, where an optimal gate decomposition of a given unitary in terms of a universal gate set is sought. Our method is related to these quantum gate compilation techniques [27–29] in seeking optima but are significantly different since the underlying unitary is also being optimized for a fixed target state.

The main insight of our work is that most optimal control techniques such as Krotov [2], GRAPE [3], CRAB [10,11], and machine learning methods [8] only require certain scalars in their update step (as opposed to a description of the entire state). We propose schemes to extract these scalars, which are either in the form of the overlap of two states $\langle\psi(t)|\chi(t)\rangle$ or the transition element between two states in a fixed Hermitian operator of the form $\langle\chi(t)|\mu|\psi(t)\rangle$ using a digital quantum simulator (DQS) and qubit measurements. A schematic illustration of our quantum-assisted quantum control algorithm can be found in Fig. 1.

Overlap estimation algorithm (OEA).—Consider two time-dependent many-body quantum states $|\psi(t)\rangle = U(t)|\psi_0\rangle$ and $|\chi(t)\rangle = V(t)|\chi_0\rangle$ generated by the evolution operators which are Trotterized implementations of a time-continuous control sequence discussed below. Given these two (generic) states, we wish to estimate the overlap $\langle\chi(t)|\psi(t)\rangle$. It is well known that if we were given the bipartite state $|x\rangle \coloneqq [|0\rangle|\psi(t)\rangle + |1\rangle|\chi(t)\rangle]/\sqrt{2}$, the real part of the overlap $\langle\chi(t)|\psi(t)\rangle$ can be evaluated by measuring the probability of $|1\rangle$ on the first (ancillary) qubit

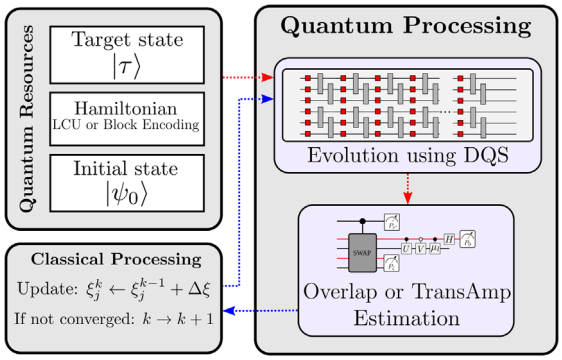

FIG. 1. A high level schematic of our quantum-assisted quantum control algorithms where scalars are extracted using digital quantum simulation combined with OEA and TAEA given target and Hamiltonian resources, provided either in terms of linear combination of unitaries (LCU) or in terms of block encoding.

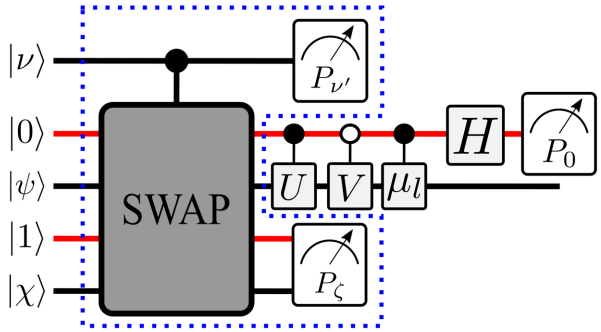

FIG. 2. A circuit for estimating transition amplitudes of the form $\langle\chi|V^\dagger\mu U|\psi_0\rangle$ using the LCU technique. Using D conditional unitaries μ_l, the transition amplitude can be estimated. The circuit inside the dotted box is an implementation of Λ_{sup} for superposing states where $|\nu'\rangle = |\langle\psi|\zeta\rangle||0\rangle + |\langle\chi|\zeta\rangle||1\rangle$.

of the state $H \otimes \mathbb{I}|x\rangle$, where H denotes the Hadamard gate. Likewise, the imaginary part of the overlap can be obtained by starting with $|x'\rangle := [|0\rangle|\psi(t)\rangle - i|1\rangle|\chi(t)\rangle]/\sqrt{2}$. We next outline a method to generate such superpositions.

To create superpositions between unknown states, we first extend the results of Oszmaniec *et al.* [30], who proposed a probabilistic completely positive (CP) map Λ_{sup} to superpose any two given states $|\psi\rangle$ and $|\chi\rangle$ which have a nonzero overlap with a given reference state $|\zeta\rangle$. Concretely, their algorithm takes as input $|\nu\rangle = \alpha|0\rangle + \beta|1\rangle, |\psi\rangle$ and $|\chi\rangle$ to generate states of the form $\alpha(\langle\psi|\zeta\rangle/|\langle\psi|\zeta\rangle|)|\psi\rangle + \beta(\langle\chi|\zeta\rangle/|\langle\chi|\zeta\rangle|)|\chi\rangle$, using well-known postselection methods [31], as incorporated in the dotted box of Fig. 2. Note that Λ_{sup} can be constructed for an arbitrary state space that $|\psi\rangle, |\chi\rangle$ lie in by using an appropriate SWAP gate and projective measurements. It is easy to see that a small error in the superposition shows up as a linear additive error in the update (see Supplemental Material [32], which includes Refs. [33–35]). If the overlaps are known, then the additional phase factor can be removed by modifying α and β appropriately. Our extension generates arbitrary superpositions of states $|\psi(t)\rangle = U(t)|\psi\rangle$ and $|\chi(t)\rangle = V(t)|\chi\rangle$ as follows. If a reference state $|\zeta\rangle$ and overlaps $\langle\chi|\zeta\rangle \neq 0$ and $\langle\psi|\zeta\rangle \neq 0$ are known, Λ_{sup} can be used to create a probabilistic superposition of the form $\alpha|0\rangle|\psi\rangle + \beta|1\rangle|\chi\rangle$ by choosing a reference state $|+\rangle|\zeta\rangle$ and inputs $|0\rangle|\psi\rangle$ and $|1\rangle|\chi\rangle$. Then by applying conditional unitaries $|0\rangle\langle 0| \otimes U(t) + |1\rangle\langle 1| \otimes V(t)$, we obtain states of the form

$$|\Psi\rangle = \alpha|0\rangle U(t)|\psi\rangle + \beta|1\rangle V(t)|\chi\rangle. \tag{1}$$

We note that superpositions of $U(t)|\psi\rangle$ and $V(t)|\phi\rangle$ can be created by applying a Hadamard on the first qubit and measuring it in the standard basis. If $\alpha = |\langle\psi|\zeta\rangle|/(\sqrt{2}\langle\psi|\zeta\rangle)$ and $\beta = |\langle\chi|\zeta\rangle|/(\sqrt{2}\langle\chi|\zeta\rangle)$, the output is the desired state $|x\rangle = [|0\rangle|\psi(t)\rangle + |1\rangle|\chi(t)\rangle]/\sqrt{2}$. Choices of the generic quantum states specify various control algorithms discussed below. For instance, the choice of $|\psi\rangle \equiv |\psi_0\rangle$ to be the initial quantum state and $|\chi\rangle \equiv |\tau\rangle$ to be the target state respectively will specify the Krotov algorithm discussed below. This method can also be used to construct several other examples of gradient-based and gradient-free control algorithms. In all such control algorithms, we choose the reference state $|\zeta\rangle$ to be a sparse quantum state with nonzero overlap with the initial and target state. For instance, $|\zeta\rangle$ can be chosen to be a sparse initial state if it has nonzero overlap with the target state. We note that this choice of the reference state is not unique and can be chosen according to experimental convenience. This reduces the problem of superposition of two unitarily rotated states to the problem of applying arbitrary control unitary on an unknown state.

Following Zhou *et al.* [36] we can add control to arbitrary unitaries U and V by padding them with controlled-X_a or internal-SWAP gates. The X_a gate has been experimentally demonstrated for photonic systems [24] and requires that each qubit state be the lower energy manifold of an otherwise controllable multilevel system. This is naturally also the case for transmon qubits [37–40] and several other physical implementations of NISQ era quantum computers. For a four level system, the X_a gate is defined by the transformation rules $|0\rangle \leftrightarrow |2\rangle, |3\rangle \leftrightarrow |1\rangle$. For larger Hilbert spaces it can be defined via a SWAP gate that acts internally on subspaces of the same Hilbert space, distinguishing it from the usual SWAP gate that acts on tensor product spaces. This doubles the internal Hilbert space dimensionality of the physical qudit with the number of additional gates needed to add control scaling linearly with the number of subsystems.

Transition amplitude estimation algorithm (TAEA).— The second time series we require for the control algorithms is the estimation of transition matrix elements $\langle\chi(t)|\mu|\psi(t)\rangle$. If the control Hamiltonian μ (see below)

can be expressed as a linear combination of known unitaries (LCUs) [41] $\mu = \sum_{l=1}^{D} c_l \mu_l$, then by applying a conditional unitary μ_l on $|\Psi\rangle$ we can estimate the overlap $\langle\chi(t)|\mu_l|\psi(t)\rangle$ and hence $\langle\chi(t)|\mu|\psi(t)\rangle$. This is presented in Fig. 2 in terms of a circuit description.

Alternatively, if there exists a block encoding [42,43] B of μ, then by applying a conditional version of this unitary on $[|0\rangle|0_k\rangle|\psi(t)\rangle + |1\rangle|0_k\rangle|\chi(t)\rangle]/\sqrt{2}$, we can estimate $\langle\psi(t)|\langle 0_k|B|0_k\rangle|\chi(t)\rangle$ and hence $\langle\psi(t)|\mu|\chi(t)\rangle$ (see Supplemental Material for a formal algorithmic description of these primitives [32]).

Quantum-assisted gradient algorithms.—We now apply these algorithmic primitives to construct quantum-assisted quantum control algorithms. Consider quantum control algorithms that operate with fixed terminal time (T) such as the Krotov algorithm [2]. Without loss of generality we work with Hamiltonians of the form $H(t) = H_0 + \xi(t)\mu$ where $H_0(\mu)$ is the bare (control) Hamiltonian. The cost function in the Krotov algorithm is given by

$$J = \langle\psi(T)|Q|\psi(T)\rangle - \alpha \int_0^T dt \xi^2(t), \tag{2}$$

where $Q = |\tau\rangle\langle\tau|$ is the projector onto the target state $|\tau\rangle$. Here the integral represents the fluence of the control field $\xi(t)$ and α is a Lagrange multiplier that modulates the relative importance of the second term. The first-order variation of the cost function produces three equations of motion,

$$|\dot{\psi}^{(k)}(t)\rangle = -iH^{(k)}|\psi^{(k)}(t)\rangle, \tag{3}$$

$$|\dot{\chi}^{(k)}(t)\rangle = -iH^{(k)}|\chi^{(k)}(t)\rangle, \tag{4}$$

$$\Delta\xi^{(k)}(t) = -\frac{1}{\alpha}\mathrm{Im}\langle\chi^{(k-1)}(t)|\mu|\psi^{(k)}(t)\rangle, \tag{5}$$

which are solved iteratively subject to the boundary conditions $|\psi^{(k)}(0)\rangle = |\psi_0\rangle$ and $|\chi^{(k)}(T)\rangle = Q|\psi^{(k)}(T)\rangle$ until convergence is reached. Here $H^{(k)}(t) = H_0 + \xi^{(k)}(t)\mu$ is the time-dependent Hamiltonian with the control field $\xi^k(t)$, state $|\psi^{(k)}(t)\rangle$, and costate $|\chi^{(k)}(t)\rangle$ corresponding to the kth iteration of the algorithm. Each iteration of the solution proceeds by evolving the state and costate equations alongside computing the overlap integral. Note that the state equation Eq. (3) is specified by an initial condition whereas the costate equation Eq. (4) is specified by a terminal condition. This implies that while the state equation is evolved forward in time, the costate equation is evolved backward in time.

By using OEA and TAEA we can implement a quantum-assisted Krotov algorithm that circumvents the exponential complexity of simulating state evolution. Throughout the algorithm we only use superpositions of the form $|y\rangle = \alpha|0\rangle|\psi(0)\rangle + \beta|1\rangle|\tau\rangle$ which can be prepared as described earlier if the overlaps with respect to some reference state are known. Evolution of states is done according to Eqs. (3) and (4) via digital quantum simulation which can be done efficiently even for many-body systems. Note that since $|\chi(t)\rangle = V(t)|\chi(T)\rangle = \langle\tau|\psi(T)\rangle V(t)|\tau\rangle$, we need to estimate the scalar overlap $\langle\tau|\psi(T)\rangle$ which can be done using OEA given $|y\rangle$. To compute the control field updates $\Delta\xi^{(k)}(t)$ we employ TAEA. Other popular algorithms such as GRAPE can also be implemented in a quantum-assisted fashion (see Supplemental Material [32]). Furthermore, we note that until now the optimization has been built into the structure of the Euler-Lagrange-like equations since they were derived using a first-order variational principle. We now extend these techniques to hybrid algorithms where there is an explicit classical optimization step in the process.

Quantum-assisted gradient-free algorithms.—Besides gradient algorithms, OEA and TAEA can also be used to implement nongradient quantum control algorithms. Typically, nongradient algorithms first guess a pulse sequence that is fine-tuned over iterations to improve fidelity. Using OEA and TAEA, the same nongradient algorithms can be used for the optimization of more complicated functionals involving overlaps and transition amplitudes. Recently, Castaldo *et al.* [44] showed that such an optimization could be performed on the IBM X2.

Resource counting.—Our algorithmic primitives use m repeated single-qubit measurements to estimate scalar values, which we group into a single *experiment* and begin the complexity analysis with the number of experiments needed for several example algorithms. We then separately estimate the relationship between Trotter error, number of measurement repetitions, and the error threshold per experiment. The superposition part of either primitive requires measurements in a basis containing the reference state $|\zeta\rangle$ which can be done easily if a unitary transformation can be implemented such that it takes some standard basis state to $|\zeta\rangle$. The OEA requires two experiments, one each for estimating real and imaginary parts. The number of experiments for TAEA depends on the approach used. While block encoding only needs two experiments, LCU requires $2D$ experiments one each for the real and imaginary parts of D different terms in the LCU decomposition of the operator μ. The number of times each quantum-assisted control algorithm invokes the algorithmic primitives can be inferred simply. For each update, one TAEA experiment and two OEA experiments are needed. Quantum-assisted GRAPE requires two fidelity experiments in each update step.

We now relate the monotonic convergence requirements to error thresholds by focusing on the quantum-assisted Krotov algorithm, the extension of this analysis to other algorithms being straightforward. We consider two sources of error, the first is due to Trotterization which results in an approximate version of the unitary corresponding to time evolution being implemented. Poulin *et al.* [45] gave an

upper bound on this error and also give an estimate for the number of gates using a Solovay-Kitaev decomposition to obtain desired levels of accuracy. The second source of error is due to the finite precision arising from finite measurements described in the central limit.

The quantum-assisted Krotov algorithm is monotonically convergent up to the point where the incremental change in the cost function $\Delta J^{(k)} = J^{(k)} - J^{(k-1)}$ in an ideal implementation is comparable to the fluctuation in $\Delta J^{(k)}$ due to the two sources of errors mentioned above. Using the upper bounds on Trotterization [45] and finite measurement errors, we can compute an upper bound on the error in each Krotov update. This can further be used to provide a lower limit for $\Delta J^{(k)}$ below which convergence cannot be guaranteed (see Supplemental Material [32]). As a result, we can guarantee that the quantum-assisted Krotov algorithm remains monotonically convergent so long as the stochastically averaged change is much larger than the typical amplitude of the fluctuations,

$$\langle\langle \Delta J^{(k)} \rangle\rangle \gg 4T\varepsilon||\mu|| + 4\frac{T}{\alpha}[\xi_{\max}\varepsilon] + 4\varepsilon_{TS}, \qquad (6)$$

where T is total time of evolution, $\xi_{\max}$ is the maximum value of the control field, $\varepsilon_M, \varepsilon_{TS}$ are bounds on the measurement and Trotterization errors, respectively, and $\varepsilon = \varepsilon_M + 3\varepsilon_{TS}||\mu||/\alpha$.

Numerical simulation.—We now present simulations for the proposed quantum-assisted Krotov algorithm. The theoretical error model is based on bounds that are well known to be not tight and it is known that gate digitization can be relatively efficient [23,46]. Hence we incorporate an aggregated error model which takes into account any additive errors to the update including Trotterization errors, measurement errors, and errors in superposition. This is done by introducing a Gaussian random noise model of standard deviation e_{amp} at every update. Our simulations use standard packages [47,48] (also see Supplemental Material [32]).

We simulate transmon qubits [49,50] whose two-qubit Hamiltonian is $\hat{H}(t)/h = H_0 + V(t)$, where $H_0 = -(\omega_1/2)\hat{\sigma}_z^{(1)} - (\omega_2/2)\hat{\sigma}_z^{(2)} + 2J(\hat{\sigma}_x^{(1)}\hat{\sigma}_x^{(2)} + \hat{\sigma}_y^{(1)}\hat{\sigma}_y^{(2)})$ and $V(t) = u(t)(\hat{\sigma}_x^{(1)} + \lambda\hat{\sigma}_x^{(2)})$. Here $\hat{\sigma}$ are Pauli matrices, $\omega_1 = 1.1$ GHz, $\omega_2 = 2.1$ GHz are energy level splitting of the first and second qubits, respectively, $J = 0.2$ GHz is the effective coupling strength, $\xi(t)$ is the control field, and $\lambda = 1.1$ is the strength of the qubit-control coupling for the second qubit relative to the first. We allow the system to evolve for 25 ns under $\hat{H}(t)$, starting from the ground state $|00\rangle$ and optimize for target state $(|00\rangle + |11\rangle)/\sqrt{2}$. The result of our noisy optimization is shown in Fig. 3, where the upper four panels show the time evolution of $|00\rangle$ (blue) and $|11\rangle$ (orange) states with decreasing noise. Other examples are discussed in the Supplemental Material [32]. In all of our simulations, we see that for moderate to low levels of noise the optimization converges to within an infidelity of 10^{-3}.

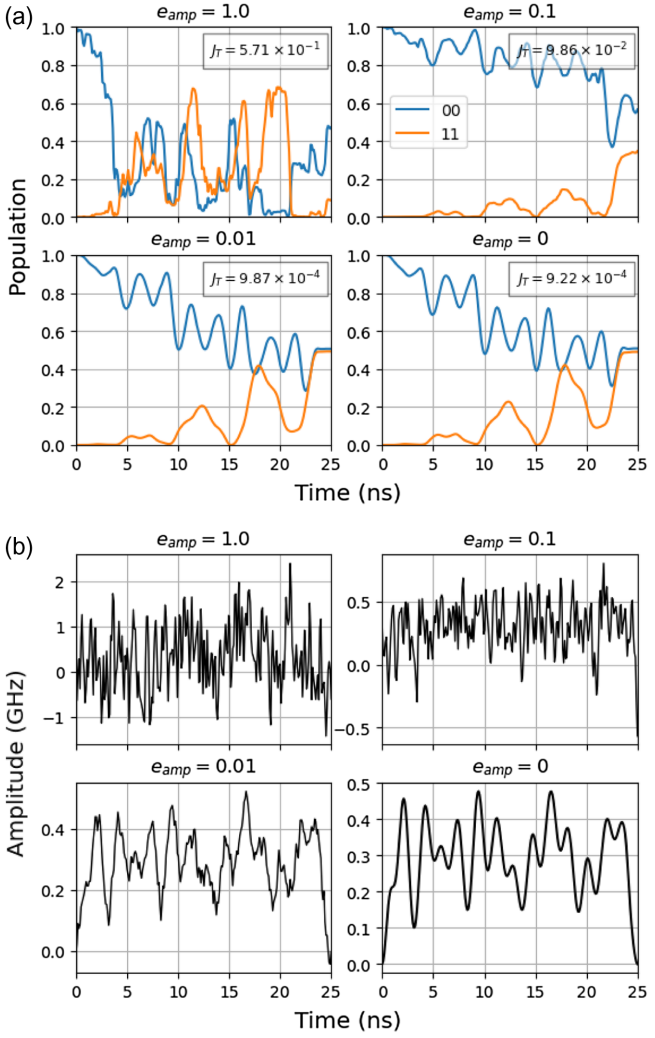

FIG. 3. Panel (a) shows how the population evolves over time along with achieved infidelity J_T for various error amplitudes e_{amp}. Panel (b) shows the corresponding optimized control pulse. The populations of $|01\rangle$ and $|10\rangle$ saturate to the expected value of 0 and are omitted for clarity.

Conclusions.—We present the algorithmic primitives OEA and TAEA to implement arbitrary quantum-assisted quantum control algorithms. Our method substantially improves existing hybrid quantum control algorithms by incorporating dense target states and complex control algorithms. Furthermore, the underlying algorithmic primitives only rely on qubit measurements and require the implementation of specific controlled unitaries, that can be accomplished by well-known methods. We emphasize that our simulations indicate that the circuit complexity of specific algorithms considered scales favorably with error thresholds. We applied our method to quantum-assisted versions of gradient and nongradient algorithms. Several

recent experiments have demonstrated control of relatively large number of qubits on differing platforms, from gradient algorithm on 12 NMR qubits [26] to a controlled state preparation of 20 transmon qubits [51] suggesting that our protocols are practical to implement with existing technology. Furthermore, when two separate platforms can both simulate the same Hamiltonians H_0 and μ, our method can be combined with analog or digital quantum simulation experiments to design optimal control pulses in new systems. For example, proposals to generate all-optical higher-dimensional tensor network states [52,53] can be used to generate complex target states for our scheme.

By introducing quantum-assisted variation of paths, our techniques add to the literature on variational quantum algorithms [54–56] and generalize the optimization program to complex overlaps which bring control theory and quantum algorithms closer [57]. Furthermore, our algorithmic primitives can also be used to optimize nongradient objectives and can be used for important tasks such as the design of modular quantum computers [58–60] and controlling reactions in quantum chemistry [61].

S. V. acknowledges support from the Government of India DST-SERB Early Career Research Award (ECR/2018/000957) and DST-QUEST Grant No. DST/ICPS/QuST/Theme-4/2019. S. V. thanks Kishor Bharti, Adolfo del Campo, Ish Dhand, Carlos Perez-Delgado, and Dario Poletti for insightful discussions.

*sai@phy.iitb.ac.in

[1] S. J. Glaser, U. Boscain, T. Calarco, C. P. Koch, W. Köckenberger, R. Kosloff, I. Kuprov, B. Luy, S. Schirmer, T. Schulte-Herbrüggen *et al.*, Eur. Phys. J. D **69**, 279 (2015).
[2] D. J. Tannor, V. Kazakov, and V. Orlov, in *Time-Dependent Quantum Molecular Dynamics* (Springer, New York, 1992), pp. 347–360.
[3] N. Khaneja, T. Reiss, C. Kehlet, T. Schulte-Herbrüggen, and S. J. Glaser, J. Magn. Reson. **172**, 296 (2005).
[4] W. Zhu and H. Rabitz, J. Chem. Phys. **109**, 385 (1998).
[5] R.-B. Wu, B. Chu, D. H. Owens, and H. Rabitz, Phys. Rev. A **97**, 042122 (2018).
[6] Q.-M. Chen, X. Yang, C. Arenz, R.-B. Wu, X. Peng, I. Pelczer, and H. Rabitz, Phys. Rev. A **101**, 032313 (2020).
[7] X.-d. Yang, C. Arenz, I. Pelczer, Q.-M. Chen, R.-B. Wu, X. Peng, and H. Rabitz, Phys. Rev. A **102**, 062605 (2020).
[8] E. Zahedinejad, J. Ghosh, and B. C. Sanders, Phys. Rev. Applied **6**, 054005 (2016).
[9] R. J. Spiteri, M. Schmidt, J. Ghosh, E. Zahedinejad, and B. C. Sanders, New J. Phys. **20**, 113009 (2018).
[10] T. Caneva, T. Calarco, and S. Montangero, Phys. Rev. A **84**, 022326 (2011).
[11] N. Rach, M. M. Müller, T. Calarco, and S. Montangero, Phys. Rev. A **92**, 062343 (2015).
[12] P. Palittapongarnpim, P. Wittek, E. Zahedinejad, S. Vedaie, and B. C. Sanders, Neurocomputing **268**, 116 (2017).
[13] A. Pechen and H. Rabitz, Phys. Rev. A **73**, 062102 (2006).
[14] S. Grivopoulos and B. Bamieh, in *Proceedings of the 42nd IEEE International Conference on Decision and Control* (IEEE, New York, 2003), IEEE Cat. No. 03CH37475, Vol. 1, pp. 434–438.
[15] R. S. Judson and H. Rabitz, Phys. Rev. Lett. **68**, 1500 (1992).
[16] M. H. Goerz, K. B. Whaley, and C. P. Koch, Eur. Phys. J. Quantum Technol. **2**, 21 (2015).
[17] D. J. Egger and F. K. Wilhelm, Phys. Rev. Lett. **112**, 240503 (2014).
[18] Y.-C. Yang, S. N. Coppersmith, and M. Friesen, Phys. Rev. A **100**, 022337 (2019).
[19] G. Jäger, D. M. Reich, M. H. Goerz, C. P. Koch, and U. Hohenester, Phys. Rev. A **90**, 033628 (2014).
[20] P. Doria, T. Calarco, and S. Montangero, Phys. Rev. Lett. **106**, 190501 (2011).
[21] S. Boixo, S. V. Isakov, V. N. Smelyanskiy, R. Babbush, N. Ding, Z. Jiang, M. J. Bremner, J. M. Martinis, and H. Neven, Nat. Phys. **14**, 595 (2018).
[22] E. Pednault, J. A. Gunnels, G. Nannicini, L. Horesh, T. Magerlein, E. Solomonik, and R. Wisnieff, arXiv:1710.05867.
[23] A. B. Magann, M. D. Grace, H. A. Rabitz, and M. Sarovar, Phys. Rev. Research **3**, 023165 (2021).
[24] J. Li, X. Yang, X. Peng, and C.-P. Sun, Phys. Rev. Lett. **118**, 150503 (2017).
[25] B. Dive, A. Pitchford, F. Mintert, and D. Burgarth, Quantum **2**, 80 (2018).
[26] D. Lu, K. Li, J. Li, H. Katiyar, A. J. Park, G. Feng, T. Xin, H. Li, G. Long, A. Brodutch *et al.*, npj Quantum Inf. **3**, 45 (2017).
[27] N. Yu, R. Duan, and M. Ying, Phys. Rev. A **88**, 010304(R) (2013).
[28] J. J. Vartiainen, M. Möttönen, and M. M. Salomaa, Phys. Rev. Lett. **92**, 177902 (2004).
[29] V. V. Shende, S. S. Bullock, and I. L. Markov, IEEE Trans. Comput. Aided Des. Integr. Circ. Syst. **25**, 1000 (2006).
[30] M. Oszmaniec, A. Grudka, M. Horodecki, and A. Wójcik, Phys. Rev. Lett. **116**, 110403 (2016).
[31] K. Li, G. Long, H. Katiyar, T. Xin, G. Feng, D. Lu, and R. Laflamme, Phys. Rev. A **95**, 022334 (2017).
[32] See Supplemental Material at http://link.aps.org/supplemental/10.1103/PhysRevLett.127.220504 for (a) details of algorithmic primitives, (b) analysis of quantum-assisted GRAPE algorithm, (c) uniform convergence threshold for KROTOV algorithm and (d) numerical simulations.
[33] N. Suri, F. C. Binder, B. Muralidharan, and S. Vinjanampathy, Eur. Phys. J. Special Topics **227**, 203 (2018).
[34] G. V. Policharla, Noisy-Krotov, https://github.com/guruvamsi-policharla/noisy-krotov.
[35] H. Buhrman, R. Cleve, J. Watrous, and R. de Wolf, Phys. Rev. Lett. **87**, 167902 (2001).
[36] X.-Q. Zhou, T. C. Ralph, P. Kalasuwan, M. Zhang, A. Peruzzo, B. P. Lanyon, and J. L. O'brien, Nat. Commun. **2**, 413 (2011).
[37] J. Koch, T. M. Yu, J. Gambetta, A. A. Houck, D. I. Schuster, J. Majer, A. Blais, M. H. Devoret, S. M. Girvin, and R. J. Schoelkopf, Phys. Rev. A **76**, 042319 (2007).
[38] J. M. Gambetta, A. A. Houck, and A. Blais, Phys. Rev. Lett. **106**, 030502 (2011).

[39] A. Mezzacapo, L. Lamata, S. Filipp, and E. Solano, Phys. Rev. Lett. **113**, 050501 (2014).
[40] T. Roy, S. Kundu, M. Chand, S. Hazra, N. Nehra, R. Cosmic, A. Ranadive, M. P. Patankar, K. Damle, and R. Vijay, Phys. Rev. Applied **7**, 054025 (2017).
[41] A. M. Childs and N. Wiebe, Quantum Inf. Commun. **12**, 0901 (2012), https://dl.acm.org/doi/10.5555/2481569.2481570.
[42] G. H. Low and I. L. Chuang, Quantum **3**, 163 (2019).
[43] A. Gilyén, Y. Su, G. H. Low, and N. Wiebe, in *Proceedings of the 51st Annual ACM SIGACT Symposium on Theory of Computing (STOC 2019)* (Association for Computing Machinery, New York, 2019), pp. 193–204, https://doi.org/10.1145/3313276.3316366.
[44] D. Castaldo, M. Rosa, and S. Corni, Phys. Rev. A **103**, 022613 (2021).
[45] D. Poulin, A. Qarry, R. Somma, and F. Verstraete, Phys. Rev. Lett. **106**, 170501 (2011).
[46] M. Heyl, P. Hauke, and P. Zoller, Sci. Adv. **5**, eaau8342 (2019).
[47] M. H. Goerz, D. Basilewitsch, F. Gago-Encinas, M. G. Krauss, K. P. Horn, D. M. Reich, and C. P. Koch, SciPost Phys. **7**, 080 (2019).
[48] J. R. Johansson, P. D. Nation, and F. Nori, Comput. Phys. Commun. **183**, 1760 (2012).
[49] P. Watts, J. Vala, M. M. Müller, T. Calarco, K. B. Whaley, D. M. Reich, M. H. Goerz, and C. P. Koch, Phys. Rev. A **91**, 062306 (2015).
[50] M. H. Goerz, G. Gualdi, D. M. Reich, C. P. Koch, F. Motzoi, K. B. Whaley, J. Vala, M. M. Müller, S. Montangero, and T. Calarco, Phys. Rev. A **91**, 062307 (2015).
[51] C. Song, K. Xu, H. Li, Y.-R. Zhang, X. Zhang, W. Liu, Q. Guo, Z. Wang, W. Ren, J. Hao, H. Feng, H. Fan, D. Zheng, D.-W. Wang, H. Wang, and S.-Y. Zhu, Science **365**, 574 (2019).
[52] M. Lubasch, A. A. Valido, J. J. Renema, W. S. Kolthammer, D. Jaksch, M. S. Kim, I. Walmsley, and R. García-Patrón, Phys. Rev. A **97**, 062304 (2018).
[53] I. Dhand, M. Engelkemeier, L. Sansoni, S. Barkhofen, C. Silberhorn, and M. B. Plenio, Phys. Rev. Lett. **120**, 130501 (2018).
[54] S. Khatri, R. LaRose, A. Poremba, L. Cincio, A. T. Sornborger, and P. J. Coles, Quantum **3**, 140 (2019).
[55] Z.-C. Yang, A. Rahmani, A. Shabani, H. Neven, and C. Chamon, Phys. Rev. X **7**, 021027 (2017).
[56] C. Lin, Y. Wang, G. Kolesov, and U. Kalabić, Phys. Rev. A **100**, 022327 (2019).
[57] A. B. Magann, C. Arenz, M. D. Grace, T.-S. Ho, R. L. Kosut, J. R. McClean, H. A. Rabitz, and M. Sarovar, PRX Quantum **2**, 010101 (2021).
[58] S. J. Devitt, A. G. Fowler, A. M. Stephens, A. D. Greentree, L. C. Hollenberg, W. J. Munro, and K. Nemoto, New J. Phys. **11**, 083032 (2009).
[59] C. Arenz and H. Rabitz, Phys. Rev. Lett. **120**, 220503 (2018).
[60] J. Lee, C. Arenz, D. Burgarth, and H. Rabitz, J. Phys. A **53**, 125304 (2020).
[61] A. Peruzzo, J. McClean, P. Shadbolt, M.-H. Yung, X.-Q. Zhou, P. J. Love, A. Aspuru-Guzik, and J. L. O'brien, Nat. Commun. **5**, 4213 (2014).